Published OnlineFirst March 29, 2011; DOI:10.1158/1535-7163.MCT-10-0695

Molecular Cancer Therapeutics

Evasion Mechanisms to Igf1r Inhibition in Rhabdomyosarcoma

Jinu Abraham[1,2], Suresh I. Prajapati[1], Koichi Nishijo[1], Beverly S. Schaffer[1], Eri Taniguchi[1], Aoife Kilcoyne[1,3], Amanda T. McCleish[1], Laura D. Nelon[1], Francis G. Giles[3], Argiris Efstratiadis[4], Robin D. LeGallo[5], Brent M. Nowak[6], Brian P. Rubin[7], Suman Malempati[2], and Charles Keller[1,2]

Abstract

Inhibition of the insulin-like growth factor 1 receptor (Igf1r) is an approach being taken in clinical trials to overcome the dismal outcome for metastatic alveolar rhabdomyosarcoma (ARMS), an aggressive muscle cancer of children and young adults. In our study, we address the potential mechanism(s) of Igf1r inhibitor resistance that might be anticipated for patients. Using a genetically engineered mouse model of ARMS, validated for active Igf1r signaling, we show that the prototypic Igf1r inhibitor NVP-AEW541 can inhibit cell growth and induce apoptosis *in vitro* in association with decreased Akt and Mapk phosphorylation. However, drug resistance *in vivo* is more common and is accompanied by Igf1r overexpression, Mapk reactivation, and Her2 overexpression. Her2 is found to form heterodimers with Igf1r in resistant primary tumor cell cultures, and stimulation with Igf2 leads to Her2 phosphorylation. The Her2 inhibitor lapatinib cooperates with NVP-AEW541 to reduce Igf1r phosphorylation and to inhibit cell growth even though lapatinib alone has little effect on growth. These results point to the potential therapeutic importance of simultaneous targeting of Igf1r and Her2 to abrogate resistance. *Mol Cancer Ther; 10(4); 697–707. ©2011 AACR.*

Introduction

Rhabdomyosarcoma (RMS) is an aggressive muscle cancer and the most common soft tissue sarcoma of childhood (1). This malignancy is a paradigm for refractory and incurable solid tumors at all ages because more than half of children with RMS at diagnosis have either regional lymph node or distant metastases (2). RMS has 2 major subtypes, alveolar rhabdomyosarcoma (ARMS) and embryonal rhabdomyosarcoma. The prognosis for children with metastatic ARMS is dismal and has been largely unchanged for decades despite tremendous advances in surgical technique, radiation therapy, and chemotherapy intensification (3, 4). An exciting approach to the treatment of metastatic ARMS in the current Children's Oncology Group trial, ARST08P1, is the addition of a molecular targeted therapy to conventional chemotherapy. The therapeutic agent in this trial is IMC-A12, a fully human IgG1 monoclonal antibody (5) targeting insulin-like growth factor 1 receptor (Igf1r), which is a receptor tyrosine kinase (RTK) that is overexpressed in RMS (6–8).

Insulin-like growth factor (IGF) signaling has a long precedent of relevance in ARMS. Our study examining gene expression profiles for RMS samples from the Intergroup Rhabdomyosarcoma Study-IV was the first to show that the IGF signaling axis is associated with decreased disease-free survival in RMS (9). Complementary studies using primary tumor samples and cell lines have shown similarly that the level of IGF signaling is increased in RMS (6, 7). Mechanistic studies suggest that the primary receptor for IGF ligands, Igf1r, is a transcriptional target of Pax3:Fkhr, which is the chimeric protein formed as a result of a reciprocal chromosomal translocation found in most ARMS (10). Furthermore, *in vivo* and *in vitro* studies using Igf1r monoclonal antibodies (11–13), Igfr-1 inhibitors (14, 15), and antisense technology (16) have shown that Igfr-1 is functionally important for tumor cell growth and cancer cell proliferation in RMS. RTKs have been targeted successfully in several cancers (17, 18). However, experience with RTK inhibitors shows that resistance and/or alternative signaling pathways can evolve in nearly a third of all tumors, thereby limiting efficacy of therapies targeting a single protein responsible

Authors' Affiliations: [1]Greehey Children's Cancer Research Institute, University of Texas Health Science Center, San Antonio, Texas; [2]Department of Pediatrics, Oregon Health and Science University, Portland, Oregon; [3]Department of Medicine, University of Texas Health Science Center, San Antonio, Texas; [4]Department of Genetics and Development, Columbia University, New York, New York; [5]Department of Pathology, University of Virginia, Charlottesville, Virginia; [6]Department of Mechanical Engineering, University of Texas, San Antonio, Texas; and [7]Department of Anatomic Pathology, Cleveland Clinic, Taussig Cancer Center and the Lerner Research Institute, Cleveland, Ohio

Note: Supplementary material for this article is available at Molecular Cancer Therapeutics Online (http://mct.aacrjournals.org/).

Corresponding Author: Charles Keller, Pediatric Cancer Biology Program, Pape' Family Pediatric Research Institute, Department of Pediatrics, Oregon Health and Science University, 3181 S.W. Sam Jackson Park Road, Mail Code L321, Portland, OR 97239-3098. Phone: (503)494-1210; Fax: (503)418-5044. E-mail: keller@ohsu.edu

doi: 10.1158/1535-7163.MCT-10-0695

Published OnlineFirst March 29, 2011; DOI:10.1158/1535-7163.MCT-10-0695

for tumor maintenance and progression (19, 20). Despite the potential impact of Igf1r inhibition, we expect resistance to evolve in a subset of patients. In this study, we use the prototypic Igf1r inhibitor, NVP-AEW541, to investigate the mechanism(s) of resistance that evolve *in vivo* using a genetically engineered mouse model of ARMS (21).

Materials and Methods

Human tissue

All human tissue was obtained by means of an Institutional Review Board approved study from the pediatric cooperative human tissue network under the Institutional Review Board approval.

Western blotting

For Western blotting, tumor tissues from mice were collected in radioimmunoprecipitation (RIPA) buffer supplemented with a cocktail of protease inhibitors and Serine/Threonine and Tyrosine phosphatase inhibitors (Thermo Fisher Scientific). Tumors were then homogenized by a nonfoaming homogenizer for 1 minute and then the lysate was centrifuged at 13,000 rpm for 10 minutes. Protein supernatants were separated by SDS–PAGE at 150 V. Proteins were then transferred onto a polyvinylidene difluoride membrane at 100 V for 1 hour. The membrane was subsequently blocked with 5% nonfat skim milk or 5% bovine serum albumin in TBS-T (TBS with 0.1% Tween 20) and then incubated with primary antibody at 4°C overnight. The following primary antibodies were used: Rabbit anti-p70 S6 kinase-α (catalogue no. sc-230; Santa Cruz Biotechnology), mouse anti-insulin receptor-β (catalogue no. sc-57342; Santa Cruz Biotechnology), rabbit anti-IRS-1 (catalogue no. sc-7200; Santa Cruz Biotechnology), rabbit anti-caspase-3 (catalogue no. 9662; Cell Signaling Technology), rabbit anti-p44/42 mitogen activated protein kinase (MAPK; Erk1/2; catalogue no. 9102; Cell Signaling Technology), rabbit anti-IGF-1 receptor-β (catalogue no. 3027; Cell Signaling Technology), rabbit anti-Akt (catalogue no. 9272; Cell Signaling Technology), rabbit anti-EGF receptor (catalogue no. 2232; Cell Signaling Technology), rabbit anti-phospho-p70 S6 kinase (Thr389; catalogue no. 9205; Cell Signaling Technology), rabbit anti-phospho-IRS-1 (Tyr632; catalogue no. sc-17196; Santa Cruz Biotechnology), rabbit anti-phospho-p44/42 MAPK (Erk1/2; catalogue no. 9101; Cell Signaling Technology), rabbit anti-phospho-Akt (Ser473; catalogue no. 4058; Cell Signaling Technology), rabbit anti-phospho-Igf1r (Tyr1161; catalogue no. sc-101703; Santa Cruz Biotechnology), or rabbit anti-phospho-Her2 (catalogue no. sc-12352-R, Santa Cruz Biotechnology). After washing with TBS-T, the membrane was incubated with the appropriate peroxidase-conjugated secondary antibody (Vector Laboratories) at 1:5,000 dilution. Chemiluminescence was then detected using SuperSignal West Pico chemiluminescent substrate or SuperSignal West Dura extended duration substrate (Pierce Biotechnology) by autoradiography or filmless luminescence detection with a Xenogen IVIS-Spectrum system (Caliper; Xenogen).

Immunoprecipitation

Cells were lysed in RIPA buffer supplemented with a cocktail of protease inhibitors and Serine/Threonine and Tyrosine phosphatase inhibitors. Total protein lysate (350 μg) was incubated with 1 μg of anti-Her2 antibody (catalogue no. OP15; Calbiochem) or 1 μg of mouse IgG1 (catalogue no. 14-4714-85; eBioscience) and rotated for 4 hours in a cold room followed by incubation with Protein A Sepharose CL-4B beads (catalogue no. 17-0780-01; GE Healthcare Biosciences) with gentle rotation at 4°C overnight. The beads were then washed thrice with cold RIPA buffer supplemented with protease and phosphatase inhibitors, resuspended in 30 μL of sample buffer and boiled at 95°C for 5 minutes. Finally, the beads were centrifuged and the supernatant was immunoblotted to detect Igf1r with anti-IGF-1 receptor-β antibody (catalogue no. 3027; Cell Signaling Technology).

IGF2 stimulation

The cells were starved overnight in serum-free medium and then they were stimulated for 30 minutes with 50 and 100 ng/mL IGF2 (R&D Systems). After 30 minutes, cells were washed with cold PBS and were then lysed in RIPA buffer supplemented with a cocktail of protease inhibitors and Serine/Threonine and Tyrosine phosphatase inhibitors. Cell lysates were then used for immunoblotting to detect phospho-Her2 using an anti-phospho-Her2 antibody (catalogue no. sc-12352-R, Santa Cruz Biotechnology).

Immunohistochemistry

The tumor samples from mice were fixed in 10% buffered formalin and then embedded in paraffin. Immunohistochemistry was done by using rabbit anti-Igf1r antibody (catalogue no. 3027; Cell Signaling Technology) at a dilution of 1:50. Custom Human tissue microarrays were generated by coauthor R.D. LeGallo.

Mouse primary tumor cell cultures

Fresh tumor tissue from mice were cut into small pieces and suspended in Dulbecco's Modified Eagle's Medium (DMEM) containing collagenase (1 mg/mL) at 37°C for 12 hours. The collagenase containing medium was then removed and the dissociated tumor cells were plated in fresh DMEM supplemented with 10% fetal bovine serum, penicillin (100 U/mL), streptomycin (100μg/mL; Invitrogen) at 37°C with 5% CO_2 in the incubator. The NVP-AEW541 innately resistant primary tumor cell cultures U35429 and U44676 have been derived from tumors that have been authenticated by a board certified pathologist. Primary tumor cell cultures U20325 and U21089 were previously described (22). C2C12 murine myoblasts were obtained from the American Type Culture Collection. The structures of NVP-AEW541 and lapatinib are given in Supplementary Fig. S1A and B,

Published OnlineFirst March 29, 2011; DOI:10.1158/1535-7163.MCT-10-0695

respectively. For treatment of primary cell cultures these drugs were dissolved in dimethyl sulfoxide (DMSO).

Cell viability assays

Mouse rhabdomyosarcoma cells were plated in a 96-well plate at 5,000 cells/well. After 18 to 24 hours, the Igf1r tyrosine kinase inhibitor, NVP-AEW541 (Novartis) and/or lapatinib (catalogue no. S1028; Selleck Chemicals) was added to the cells at varying concentrations. After growing the cells for 72 hours in the presence of the drug, the effect of the drug on tumor cells was assessed by using CellTiter-Glo Luminescent Cell Viability Assay (Promega) and a SpectraMax M5 luminometer (Molecular Devices).

Colony formation assays

For anchorage-dependent colony formation assays, mouse rhabdomyosarcoma cells were plated in a 6-well plate at 500 cells/well. After 24 hours, NVP-AEW541 was added to the wells at varying concentrations. The cells were allowed to grow in the presence of NVP-AEW541 for 8 days and then the colonies were fixed in methanol and visualized after staining with Giemsa. For soft agar assays, 2 mL of 1.4% agarose in complete medium was poured into the wells of a 6-well plate. In each well, 5,000 cells were suspended in 2 mL of 0.7% agarose (at 37°C) in complete medium in the presence or absence of NVP-AEW541. The cells in agarose were plated atop a 1.4% agarose layer and were allowed to grow for 3 weeks before visualizing the colonies by light microscopy.

In vivo studies

All animals were treated humanely and the experiments were conducted in accordance with the Institutional Animal Care and Use Committee approved protocols. A detailed description of the transgenic mouse model of alveolar rhabdomyosarcoma has been previously reported (21, 23). The length, width, and height of the tumors were measured with a digital calipers and the tumor volume was calculated from the formula $\pi/6 \times$ length $\times$ width $\times$ height. The tumor-bearing mice were treated with NVP-AEW541 (Novartis) at a dose of 50 mg/kg/12 hours by oral gavage (enterally). After 2 weeks of treatment, the mice were euthanized and the tumor was harvested for further analysis.

Growth of ARMS cells on quail chorioallantoic membrane

Fertilized quail eggs were purchased from Boyd's Birds Co. Eggs were washed with water, dried, sprayed with 70% ethanol, and incubated at 37.4°C until embryonic day 3 (E3). Forceps were used to remove a small portion of the shell and the contents of the egg were transferred to a well of a 6-well plate. At E6, 1×10^6 alveolar rhabdomyosarcoma cells grown on a 3D scaffold (3D Biotek) were added to the chorioallantoic membrane (CAM). Cells of this primary tumor cell culture from our Pax3:Fkhr, p53 mouse model also harbor a genetically engineered luciferase gene that allow their detection and quantification (24). The day following xenoplantation, 20 μL of complete medium containing 10 μmol/L NVP-AEW541 or 100 μmol/L imatinib was added to the cells.

Quantification of drug response of ARMS cells on the quail CAM

Three days after adding the drug to the cells, 400 μL of 1.5 mg/mL luciferin diluted in PBS was added dropwise to the surface of the CAM. After 30 minutes, the quail embryo was imaged using a Xenogen IVIS-Spectrum system (Caliper; Xenogen). The image acquisition parameters were 10 seconds exposure time, 4 × 4 binning, 4-cm field of view, and f/stop of 1. Images were analyzed using Living Image 3.2 (Caliper; Xenogen). The intensity of the signal correlated with cell number (Supplementary Fig. S2A, $r^2 = 0.983$ for U48484) and was used as a surrogate for cell number in subsequent experiments.

Statistical analysis

Student's *t*-tests were done for determining statistical significance in gene expression studies and probability value of less than 0.05 was accepted as significant. Wherever applicable all the experiments were done in triplicates and repeated twice unless mentioned otherwise.

Results

Igf1r and *Igf2* are overexpressed in human and mouse alveolar rhabdomyosarcoma

To compare the mRNA expression level of *IGF1R* and its ligands *IGF1* or *IGF2* in human skeletal muscle, alveolar rhabdomyosarcoma, and embryonal rhabdomyosarcoma, a quantitative reverse transcriptase (RT)-PCR was done using tumor tissue from diagnostic (clinical) biopsies and also from our immune-competent mouse model. In the case of human alveolar and embryonal rhabdomyosarcoma, the IGF receptors *IGF1R* and *IGF2R* along with their ligand *IGF2* showed significantly increased mRNA levels compared to the normal skeletal muscle (Supplementary Fig. S3A). The expression of *IGF1* in normal skeletal muscle and rhabdomyosarcoma tumors were not significantly different.

In our mouse model, we observed a significant increase in *Igf1r* for both the primary and metastatic tumor tissue compared to the normal skeletal muscle, whereas the levels of *Igf2* and *Igf2r* were significantly elevated only in the tumor samples. Preneoplastic tissue showed very low expression of IGF ligands and receptors (Supplementary Fig. S3B). Together these results suggest that overexpression of *Igf1r* and *Igf2* but not *Igf1* may play a differential role in the initiation and progression of alveolar rhabdomyosarcoma.

Igf1r is expressed and activated in human and mouse alveolar rhabdomyosarcoma

To confirm our RT-PCR data, we did immunohistochemistry for Igf1r on human and mouse rhabdomyosarcoma

Published OnlineFirst March 29, 2011; DOI:10.1158/1535-7163.MCT-10-0695

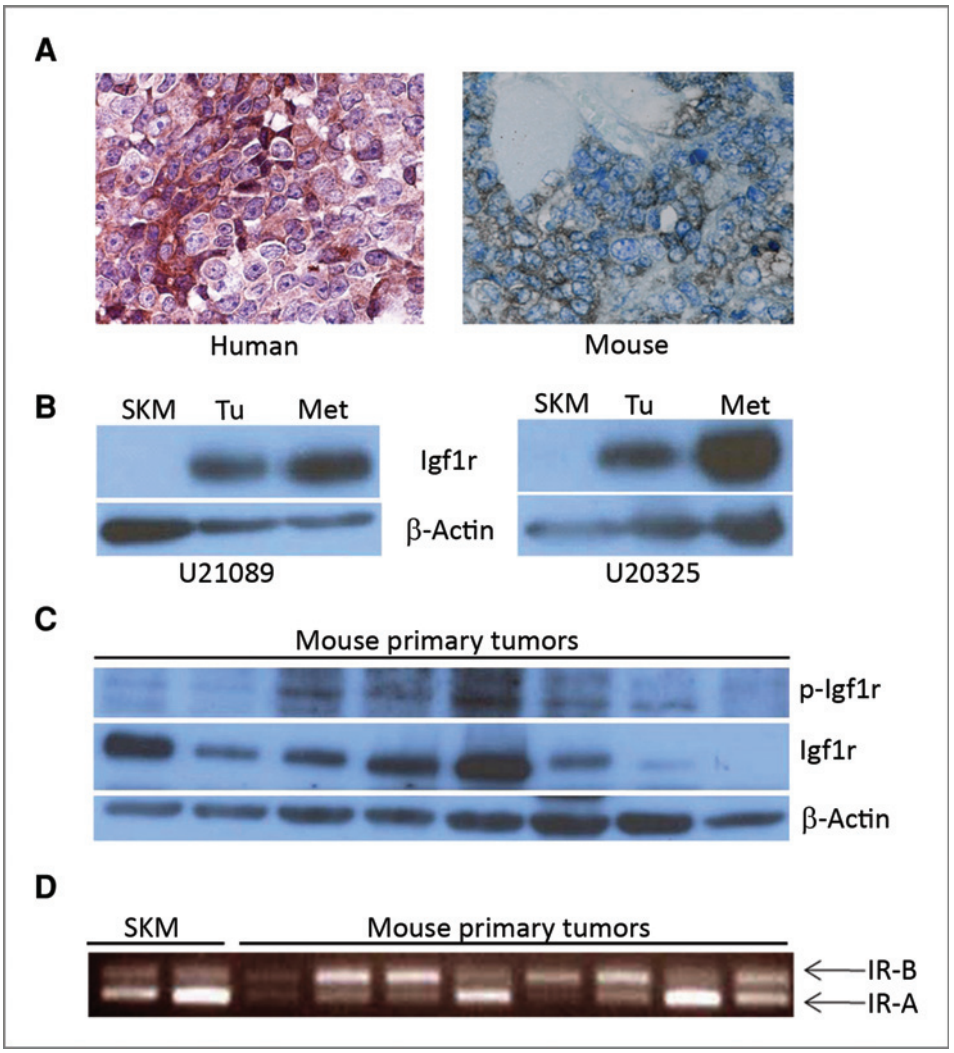

Figure 1. High expression of Igf1r in human and mouse alveolar rhabdomyosarcoma. A, immunohistochemistry for Igf1r showing tumor cells over-expressing Igf1r in primary tumors from human (top, left) and mouse (top, right) alveolar rhabdomyosarcoma. B, Western blots showing very high expression of Igf1r in the primary and metastatic tumor lysates compared to the normal skeletal muscle from the mouse model of alveolar rhabdomyosarcoma. SKM, normal skeletal muscle; Tu, primary tumor; Met, metastatic tumor. C, immunoblotting showing stochastically varied levels of Igf1r expression in the mouse tumors; most of the tumor lysates were also positive for p-Igf1r indicating that Igf1r signaling pathway was active in these mouse tumors. D, reverse transcriptase PCR showing the expression of insulin receptor isoforms IR-A and IR-B in mouse skeletal muscle and ARMS.

samples. The results showed strong focal staining for Igf1r in tumor cells without any significant staining in the surrounding stroma or myofibers (Fig. 1A). Western blotting done with murine rhabdomyosarcoma tumor and metastatic samples showed very high expression of Igf1r compared to the normal skeletal muscle (Fig. 1B). To confirm that Igf1r is activated, we did immunoblotting for phospho-Igf1r on mouse tumor lysates and cell lines, revealing that Igf1r is stochastically activated in murine tumors (Fig. 1C). We next turned to examination of expression of the Igf1r heterodimer partner, insulin receptor isoform A (IR-A). IR-A has been shown to bind Igf2 with high affinity and cause mitogenic effects; furthermore, IR-A has also been found to be overexpressed in breast and colon cancers compared to normal tissues (25). Our RT-PCR results showed that IR-A is expressed both in normal skeletal muscle and rhabdomyosarcomas from our mouse model (Fig. 1D), but not differentially. Collectively, these results validated the study of an Igf1r tyrosine-kinase inhibitor.

Treatment with *Igf1r* siRNA inhibits growth and IGF signaling

To test whether Igf1r is functionally important for tumor cell growth, we transfected a mouse primary tumor cell culture (U21089) with *Igf1r* small-interfering RNA (siRNA). Rhabdomyosarcoma cells were very sensitive to *Igf1r* siRNA whereas murine C2C12 myoblasts were not (Supplementary Fig. S4A). Western blotting confirmed significant reduction in the protein levels of Igf1r (Supplementary Fig. S4B). We also found that Igf1r knock-down caused a reduction in the phosphorylated forms of Igf1r, MAPK, Akt, IRS, and P70 S6 kinase, thereby indicating that *Igf1r* siRNA treatment prevented the activation of Igf1r signaling pathway (Supplementary Fig. S4B).

Mouse tumor cell growth is significantly inhibited by NVP-AEW541

Similar to the primary tumors from our mouse model, the tumor primary cell cultures highly expressed Igf1r at

Published OnlineFirst March 29, 2011; DOI:10.1158/1535-7163.MCT-10-0695

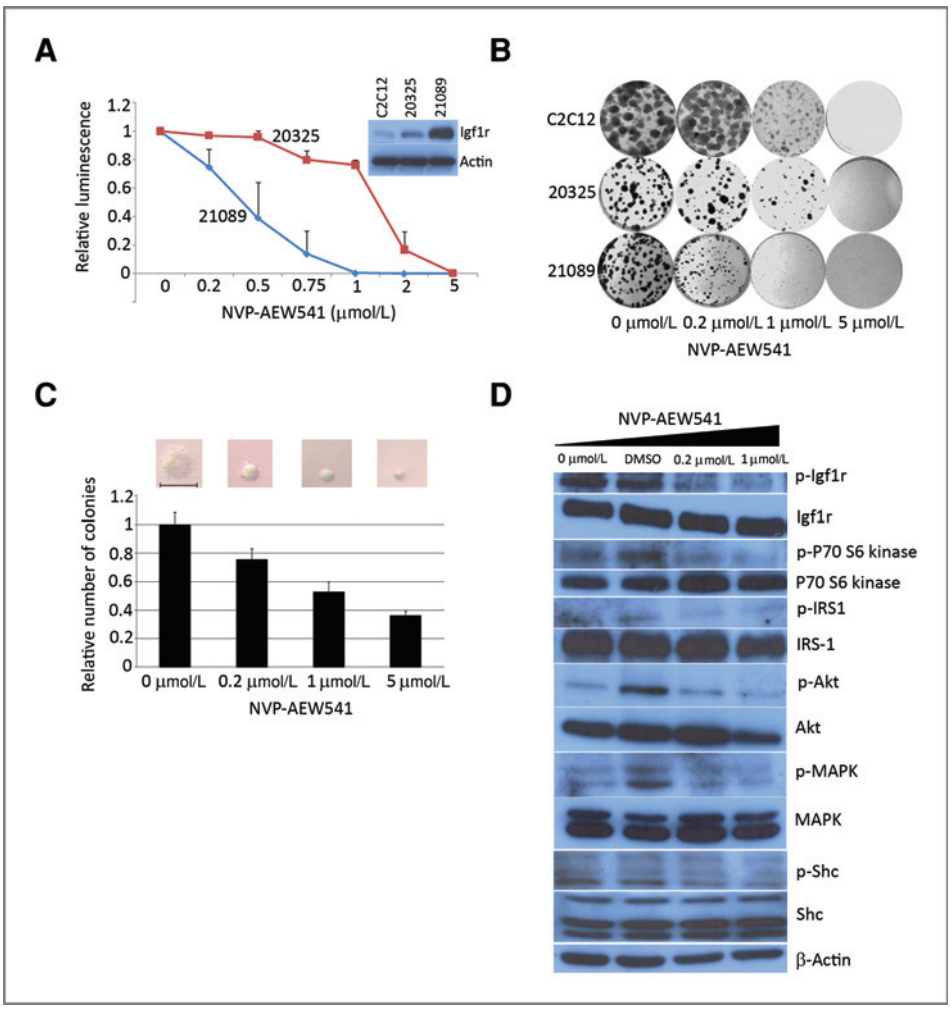

Figure 2. NVP-AEW541 inhibits the growth of mouse tumor primary cell cultures. A, cell viability assay for mouse rhabdomyosarcoma cultures treated with various doses of NVP-AEW541 and immunoblot showing expression levels of Igf1r in mouse rhabdomyosarcoma primary cell cultures (U20325 and U21089) compared with the mouse myoblast cell line C2C12. B, anchorage-dependent colony formation assay showing increased inhibition of colony formation by mouse rhabdomyosarcoma cultures compared to mouse myoblast cell line C2C12 on treatment with increasing doses of NVP-AEW541. C, anchorage-independent colony formation by mouse rhabdomyosarcoma cultures (U20325) is inhibited on treatment with NVP-AEW541, indicated by a decrease in colony size. The scale bar represents 50 μm. The number of colonies formed in soft agar also is reduced on treatment with NVP-AEW541. D, Western blot showing decrease in the phosphorylation of Igf1r, P70 S6 kinase, IRS1, Akt, Mapk, and Shc on treatment of the mouse rhabdomyosarcoma primary cell cultures (U20325) with increasing amounts of NVP-AEW541.

the protein level in comparison to the normal mouse myoblast cell line C2C12 (Fig. 2A). To examine whether an Igf1r tyrosine kinase inhibitor would affect the growth of mouse primary tumor cell cultures expressing low versus high baseline Igf1r levels, we treated the tumor cell cultures (U20325 and U21089, respectively) with NVP-AEW541 at concentrations ranging from 200 nm to 5 μmol/L. NVP-AEW541 inhibited tumor cell growth better in the primary cell culture with the higher baseline Igf1r level (IC50 1.5 μmol/L vs. 300 nmol/L for low and high Igf1r expressing cells, respectively; Fig. 2A). Anchorage-dependent colony formation assays showed that the colony forming ability of the tumor cells was drastically reduced on treatment with 1 μmol/L NVP-AEW541 (Fig. 2B), but again sensitivity was increased for the cell culture with the higher baseline level of Igf1r expression. Similar results were obtained for anchorage-independent soft agar colony formation assays (Fig. 2C). Biochemical interrogation revealed that phosphorylation of Igf1r and downstream mediators Mapk, Akt, IRS-1, and P70-S6 kinase were inhibited on treatment with NVP-AEW541 (Fig. 2D). These results suggest that Igf1r is an important mediator of tumor cell growth and proliferation and that inhibition of the Igf1r signaling axis in tumor cells is most effective when baseline Igf1r expression is elevated.

NVP-AEW541 causes cell cycle arrest and induces apoptosis in tumor cells

To determine whether the decrease in rhabdomyosarcoma cell growth *in vitro* was due to cell cycle arrest and/or induction of apoptosis, we treated primary tumor cell cultures with NVP-AEW541 for 48 hours and then performed cell cycle analysis by FACS. NVP-AEW541 treatment of mouse primary tumor cell cultures caused cell cycle arrest in G_1 phase (Fig. 3A). The proportion of cells in G_1 phase increased from 52.2% in untreated cells to 68.4% cells in G_1 phase when cells were treated with 2 μmol/L NVP-AEW541 ($P < 0.05$). Western blotting showed the presence of cleaved caspase-3 in tumor cells treated with 5 μmol/L NVP-AEW541 but not at lower concentrations (Fig. 3B). These results indicate that NVP-AEW541 reduces tumor cell growth primarily by causing

Published OnlineFirst March 29, 2011; DOI:10.1158/1535-7163.MCT-10-0695

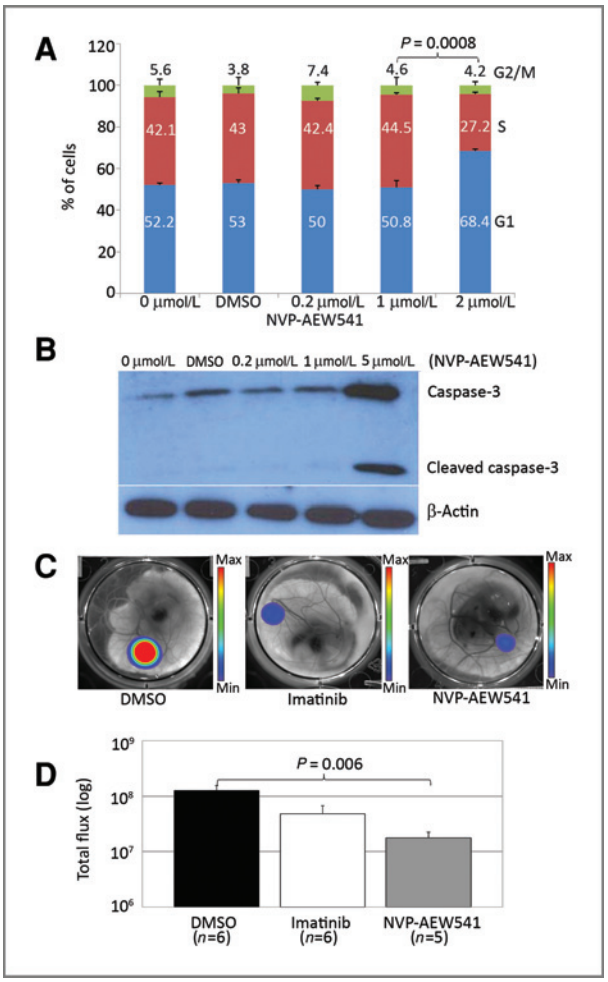

Figure 3. NVP-AEW541 induces tumor growth inhibition, cell cycle arrest, and apoptosis in primary tumor cell cultures. A, treating the mouse rhabdomyosarcoma primary cell cultures (U20325) with increasing amount of NVP-AEW541 induces cell cycle arrest in the G_1 phase. B, at moderately high concentrations of NVP-AEW541, the mouse rhabdomyosarcoma cells (U20325) show increased apoptosis as evident by the presence of cleaved caspase-3 at 5 μmol/L (but not at 2 μmol/L, unpublished data). C, representative (median) images of luminescence emitted by rhabdomyosarcoma primary cell cultures grown on quail CAM and being treated with DMSO, imatinib, and NVP-AEW541. The images are displayed with a minimum–maximum scale of 2×10^6 to 2×10^7 photons/s/cm^2/steradian. D, graphical representation of the intensity of bioluminescence signal emitted by rhabdomyosarcoma primary cell cultures grown on quail CAM that were being treated with DMSO, imatinib (100 μmol/L), or NVP-AEW541 (10 μmol/L).

cell cycle arrest and secondarily by inducing apoptosis in rhabdomyosarcoma.

NVP-AEW541 significantly inhibits the growth of tumor cells *in ovo*

To test whether NVP-AEW541 can affect the growth of rhabdomyosarcoma tumor cells grown in the context of a vascularized tissue, i.e., the quail CAM, tumor cells grown on 3D scaffolds were added to shell-free CAMs incubated in a 6-well plate format. The next day, NVP-AEW541 or control treatment (vehicle as a negative control, imatinib as a positive control) was added to the cells growing on the CAM. Since tumor cells carry a genetically engineered luciferase gene, the growth of the tumor cells could be quantified by adding luciferin to the CAM and measuring the bioluminescence 3 days after treatment (Supplementary Fig. S2A). Although quail embryo viability and growth were unaffected (Supplementary Fig. S2B), CAM harboring tumor cells treated with NVP-AEW541 showed 87% less growth compared to the DMSO treated tumor cells ($P = 0.006$), which was better than the growth inhibition seen for imatinib ($P = 0.039$) at the dosages tested (Fig. 3C and 3D). No significant difference in growth inhibition was observed in CAM harboring tumor cells treated with NVP-AEW541 compared to cells treated with imatinib ($P = 0.19$).

In vivo effect of NVP-AEW541

Since NVP-AEW541 was found to significantly inhibit proliferation in primary tumor cell cultures and by the CAM assay, we investigated the effect of NVP-AEW541 on the tumor growth and progression in our mammalian (mouse) model. Tumor-bearing mice were treated with 50 mg/kg NVP-AEW541 2 times a day by oral-gavage. Out of the 15 mice treated a majority (9) of the mice did not respond to treatment. Most of these tumors appeared to have innate/rapidly developing resistance (Fig. 4C), whereas other tumors showed initial sensitivity and but gradually evolved resistance over a several days (Fig. 4B). A minority of tumors exhibited partial response (tumor regression; Fig. 4A). A side effect commonly observed with NVP-AEW541 administration was body weight loss in the range of 10% to 20% (data not shown). These results suggest that even though targeting Igf1r might be a valid therapeutic strategy, preventing weight loss and overcoming innate or slowly evolving resistance to Igf1r tyrosine-kinase inhibitors will be crucial for this therapeutic approach in rhabdomyosarcoma.

Dissecting the resistance mechanism(s) to NVP-AEW541

To investigate the mechanism of resistance to Igf1r inhibitors, protein lysates from tumors resistant to NVP-AEW541 were subjected to immunoblotting for components of the Igf1r signaling axis as well as parallel RTKs. Surprisingly, the resistant tumor samples showed increased expression of Igf1r compared to the untreated tumor samples (Fig. 5A). The levels of other tyrosine-kinase receptors that have been implicated in Igf1r inhibitor resistance for other cancers including Her2, epidermal growth factor receptor (EGFR), and insulin-receptor were examined in the untreated and resistant samples (Fig. 5A). Stochastically increased expression levels of Her2, IR, and EGFR in the resistant samples in comparison to the untreated samples were observed. Cells from a sensitive tumor cell mass present at the end of 1-week treatment also showed significant expression of Her2, IR, and EGFR (this sample could represent a preresistant

Published OnlineFirst March 29, 2011; DOI:10.1158/1535-7163.MCT-10-0695

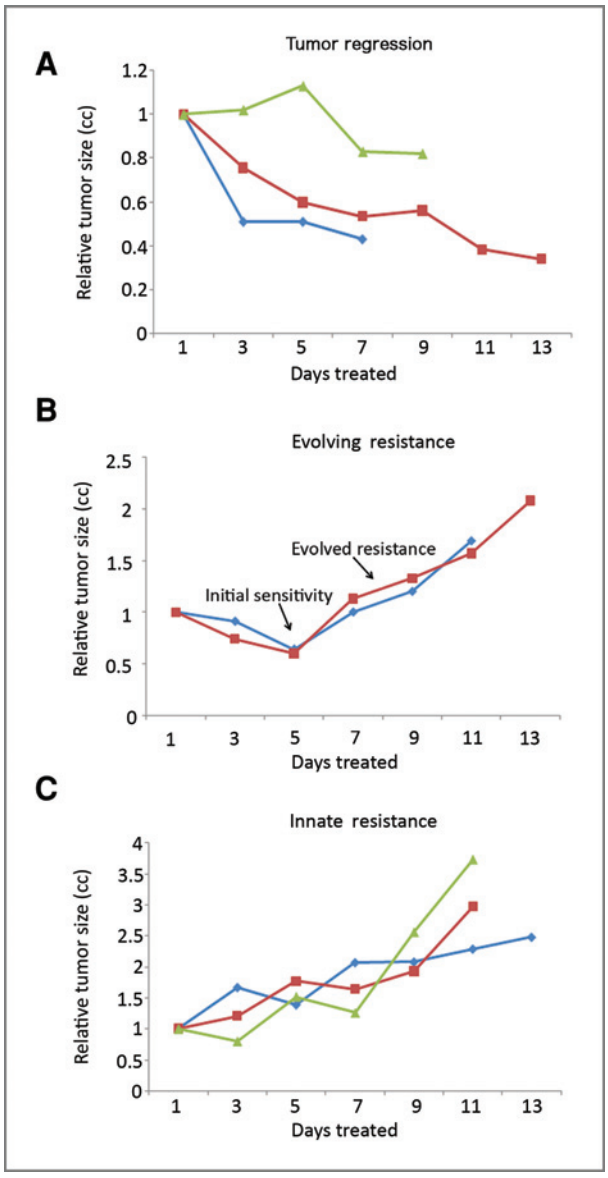

Figure 4. Effect of NVP-AEW541 on rhabdomyosarcoma *in vivo*. A, mice bearing tumors were treated with 50 mg/kg of NVP-AEW541 every 12 hours by oral gavage. This figure shows tumor bearing mice ($n = 8$) treated with NVP-AEW541 and representative of the ($n = 15$) total mice tested. A, mice that were partially sensitive to treatment (overall 3 out of 15 were sensitive). B, mice that responded to treatment initially, but slowly evolved drug resistance (3 out of 15). C, mice that showed innate (rapidly developing) resistance (9 out of 15 mice).

state). RT-PCR showed that *IR-A* was present in both in untreated and resistant tumors (Fig. 5B).

Importantly, we detected Igf1r activation in most of the resistant tumor samples, as well as a high level of p-Igf1r in the sensitive tumor that had persisted despite several days' therapy. We also found stochastic activation of MAPK signaling but not Akt in the resistant tumor samples (Fig. 5A). High MAPK activity was also observed for the sensitive tumor sample, consistent with the possibility of a preresistant state. These results led us to investigate whether resistance to NVP-AEW541 is mediated by overexpression of Igf1r and possibly through activation of MAPK, which might be the consequence of heterodimerization of Igf1r and Her2.

Her2 associates with Igf1r and is activated by Igf2

As stated above, NVP-AEW541 treated tumor lysates showed consistent overexpression of both Igf1r and Her2 receptors. To examine whether these receptors heterodimerize and to investigate whether there is crosstalk between the 2 signaling pathways, we generated 2 primary tumor cell cultures (U35429 and U44676) from our tumor samples that were innately resistant to NVP-AEW541 for use in biochemical and functional studies. Immunoprecipitation of Her2 from the NVP-AEW541 resistant cell lysates and subsequent immunoblotting with an Igf1r antibody showed that Igf1r interacts with Her2 in resistant cell cultures. Conversely, no interaction between Igf1r and Her2 was observed in a naïve (untreated) murine rhabdomyosarcoma primary cell culture (Fig. 5C). When the tumor cell lysates were immunoprecipitated with a mouse IgG1 (control), no Igf1r was detected, suggesting that the interaction between Igf1r and Her2 was specific. To investigate whether crosstalk exists between Igf1r and Her2 in the NVP-AEW541 resistant rhabdomyosarcoma cells, we serum starved cultures overnight then treated cultures with 50 or 100 ng/mL IGF2 for 30 minutes. Western blot analysis of the cells stimulated with IGF2 showed an increase in the levels of phospho-Her2 in the NVP-AEW541 resistant rhabdomyosarcoma primary cell culture but not in the naïve rhabdomyosarcoma cells (Fig 5D). These results suggest that Igf1r heterodimerizes with Her2 in NVP-AEW541 resistant rhabdomyosarcoma cells and that direct or indirect crosstalk exists between these 2 receptors.

Tyrosine-kinase inhibition of both Igf1r and Her2 has an additive effect on NVP-AEW541 resistant rhabdomyosarcoma cells

To investigate the functional significance of Igf1r overexpression and Igf1r-Her2 complex formation in NVP-AEW541 resistant rhabdomyosarcoma, we treated a NVP-AEW541 resistant rhabdomyosarcoma primary cell culture with NVP-AEW541, lapatinib (a small molecule inhibitor of Her2 and EGFR) or a combination of both for 72 hours. The results of the cell viability assay showed that NVP-AEW541 alone led to an unexpected increase in cell growth at moderate doses for the NVP-AEW541 resistant cell culture (see Discussion). However, the cell growth inhibition could be cooperatively improved by addition of lapatinib (cooperativity index 0.1), although lapatinib alone had no substantial effect on naïve or resistant tumor cells (Fig. 6A and 6B). To examine the activity of Igf1r and Her2 in NVP-AEW541 resistant primary tumor cell lines, we treated the cells with 5 μmol/L NVP-AEW541, 5 μmol/L lapatinib or their combination for 25 minutes and did Western

Published OnlineFirst March 29, 2011; DOI:10.1158/1535-7163.MCT-10-0695

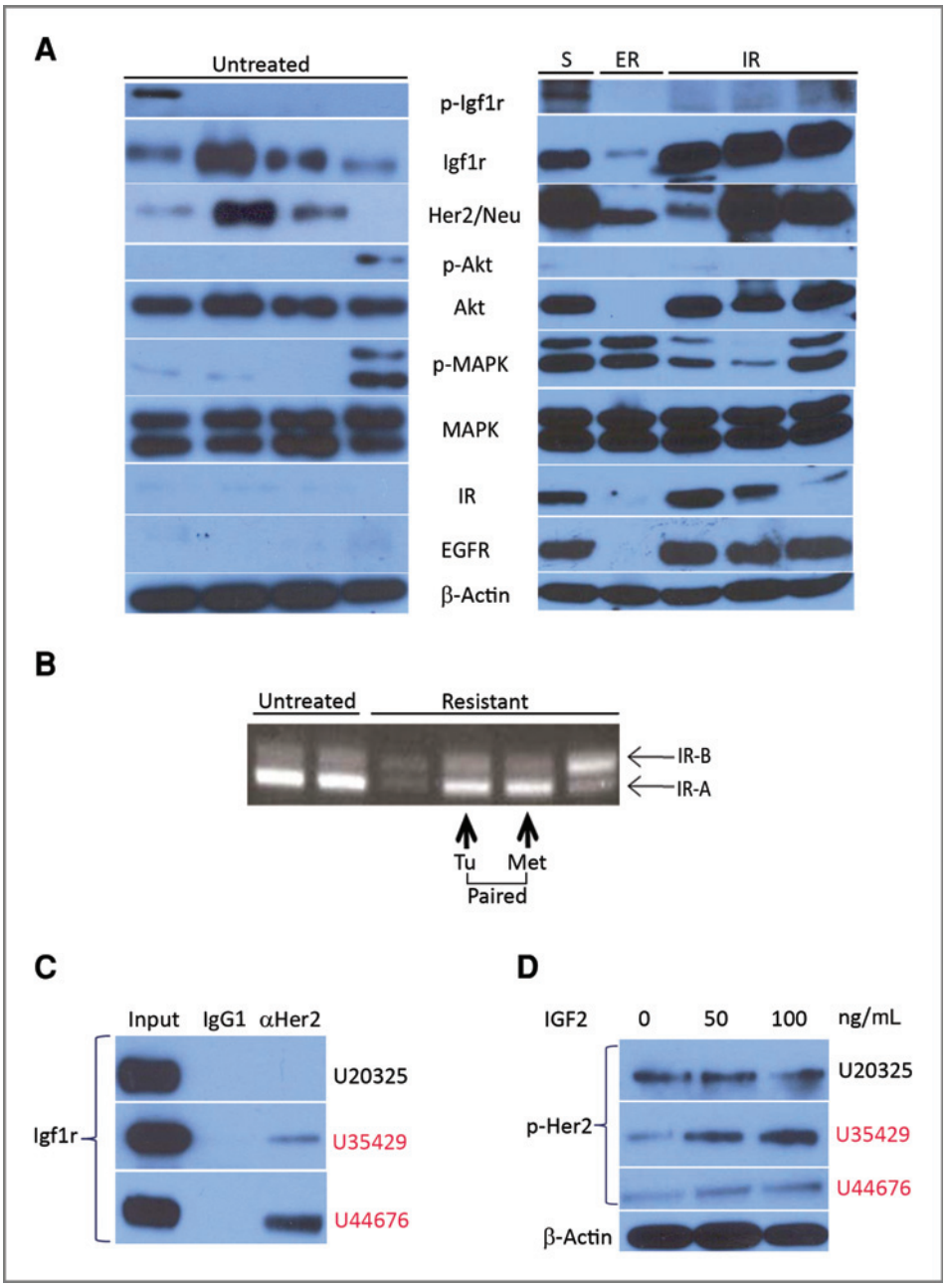

Figure 5. Investigating the mechanism of NVP-AEW541 resistance in tumors. A, Western blot analysis of tumors from untreated and NVP-AEW541 treated mice. Immunoblotting shows that mice resistant to NVP-AEW541 had stochastically increased expression of Igf1r and Her2 as well as activated Mapk signaling. S, sensitive tumor in which a residual cell mass persisted. ER, slowly evolved resistant tumor; IR, innately and rapidly resistant tumors. B, RT-PCR showing the expression pattern of the insulin receptor isoforms A and B in the untreated and NVP-AEW541 resistant mice. C, Her2 was immunoprecipitated from naïve (untreated, black) and NVP-AEW541 innately/rapidly resistant (red) rhabdomyosarcoma primary cell culture lysates and then immunoblotted to detect Igf1r. D, the NVP-AEW541 resistant and naïve rhabdomyosarcoma primary cell cultures were treated with 50 and 100 ng/mL IGF2 for 30 minutes and then the cell lysates were analyzed by Western blotting for activated (phosphorylated) Neu/Her2.

blotting for p-Her2 and p-Igf1r. Resistant cell cultures treated with lapatinib showed decreased p-Her2 levels; however, no difference in Her2 activity was observed in cells treated with NVP-AEW541. When the resistant cells were treated with lapatinib, a surprising increase in the levels of p-Igf1r was observed in comparison vehicle treated cells (Fig. 6C). This effect was not observed in naïve tumor cells (data not shown). Resistant cells treated with NVP-AEW541 still harbored detectable levels of p-Igf1r, but cells treated with the combination of lapatinib and NVP-AEW541 showed a substantial reduction in p-Igf1r. These results suggest that the combination of lapatinib and NVP-AEW541 is a feasible therapeutic strategy for abrogating resistance to Igf1r inhibitors in ARMS.

Discussion

Resistance to RTK inhibitors is known to emerge in a third of cancer cases and this resistance could arise by multiple mechanisms including RTK transcriptional overexpression, gene amplification, RTK mutation, or parallel pathway activation (26–29). Activating mutations in Igf1r responsible for conferring resistance to Igf1r

Published OnlineFirst March 29, 2011; DOI:10.1158/1535-7163.MCT-10-0695

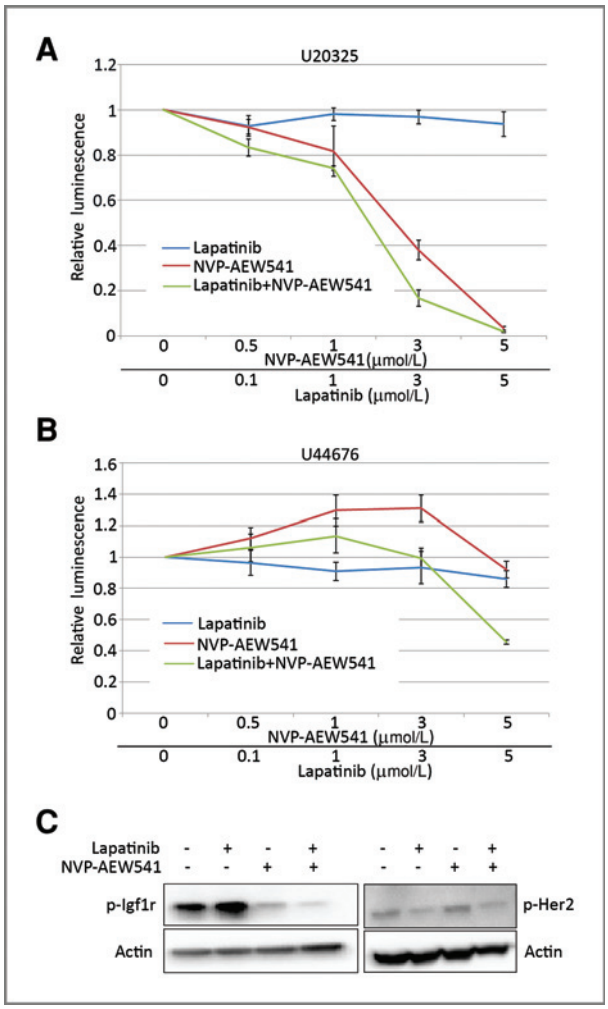

Figure 6. Combination of NVP-AEW541 and lapatinib cooperatively inhibits the growth of NVP-AEW541 resistant murine rhabdomyosarcoma primary cell cultures with Igf1r/Her2 complexes. Cell viability assay for naïve, untreated (U20325; A) and NVP-AEW541 innately resistant mouse rhabdomyosarcoma primary culture (U44676; B) treated with varying concentrations of NVP-AEW541, lapatinib, or a combination of both. Naïve cells (U20325) were sensitive to NVP-AEW541, but lapatinib had no cooperativity. In contrast, NVP-AEW541 at moderate doses increased cell growth in resistant cell cultures (U44676). However, this paradoxical effect was reduced by the addition of lapatinib, although lapatinib treatment alone had very little effect. C, the NVP-AEW541 resistant primary tumor cell line (U44676) was treated with DMSO, 5 μmol/L lapatinib, 5 μmol/L NVP-AEW541, and a combination of 5 μmol/L NVP-AEW541 + lapatinib for 25 minutes and Western blot analysis was done on lysates for p-Igf1r and p-Her2.

inhibitors have not been reported, but in some cancers Hsp90 has been found to stabilize Igf1r and thus confer resistance to anti-Igf1r treatment (30) and in other cases differential IGF binding protein expression has altered ligand stability and led to resistance to Igf1r small-molecule inhibitors (31). A recent report of a drug-selected rhabdomyosarcoma cell line has also shown the possibility that PDGFR-A can confer resistance to an Igf1r small molecule inhibitor through receptor switching (32). However, this resistance mechanism was not observed *in vivo* in our Igf1r inhibitor studies, despite the important role of Pdgfr-a as an *a priori* therapeutic target that we have established in this same model (22).

Our current report adds to an emerging body of evidence highlighting the important reciprocity of Igf1r and Her2 in resistance to targeted therapies in cancer (33–39). Trastuzumab is a humanized recombinant monoclonal antibody that targets the Her2 receptor and is an Food and Drug Administration approved drug for the treatment of metastatic breast cancer (40–42), yet resistance to Trastuzumab is a very common in breast cancers overexpressing Her2 (34). One of the mechanisms leading to Trastuzumab resistance is the formation of Igf1r and Her2 heterodimers resulting in Her2 phosphorylation in Trastuzumab resistant cells (35). A caveat to the Trastuzumab example, however, is that resistance mechanism (s) may vary depending on whether Igf1r inhibition is mediated by monoclonal antibodies or tyrosine kinase inhibitors.

Reciprocal to the evidence that Igf1r can mediate Her2 resistance, other evidence shows that the HER family receptors can also mediate resistance to Igf1r inhibitors. Studies in ovarian cancer cell lines show that activation of EGFR and Her2 receptors confers resistance to a small molecule inhibitor targeting Igf1r. These ovarian cancer cells showed elevated expression and activation of the HER family receptors on treatment with the Igf1r inhibitor. Interestingly, not only did inhibition of Igf1r in the ovarian cancer cell lines lead to an increase in Her2 phosphorylation, but treatment with a pan-HER inhibitor resulted in increased Igf1r phosphorylation, suggesting a bidirectional crosstalk between these 2 pathways in ovarian cancer cells. In these studies, simultaneously targeting Igf1r and Her family receptors led to a higher degree of cell death compared to single agent therapy (33). The heteromeric association between Igf1r and Her2 has also been observed in MCF-7 human breast cancer cells, and this association was triggered by the presence of ligands heregulin and Igf1 (43).

In our study we have shown that Igf1r and Her2 interact only in those mouse rhabdomyosarcoma tumor cells that are innately (rapidly) resistant to the Igf1r inhibitor, NVP-AEW541, but not in naïve, untreated cells. An increase in Her2 phosphorylation was observed on stimulation with IGF2 only in the resistant cells, whereas there was no change in the level of phosphorylated Her2 in untreated rhabdomyosarcoma cells stimulated with IGF2. Our study suggests that while Her2 may be of some biological importance for naïve rhabdomyosarcoma tumors, Her2 may become a critical Igf1r signaling pathway adjunct for the survival of tumor cells under selection pressure by an Igf1r inhibitor.

Our results also suggest that the mechanism of Igf1r/Her2 crosstalk may be more complex than a simple receptor–receptor interaction. Since treatment with Lapatinib did not block the phosphorylation of Igf1r and instead caused an increase in phosphorylation of Igf1r,

Published OnlineFirst March 29, 2011; DOI:10.1158/1535-7163.MCT-10-0695

we speculate that yet-unidentified third party adapter molecules (possibly non-RTKs) with opposing actions may mediate Her2/Igf1r interactions in NVP-AEW541 resistant cells. Displaced from Her2 by a Her2 antagonist, these nonreceptor kinases would be free to interact with and stimulate Igf1r phosphorylation. Studies by Belsches-Jablonski and colleagues have shown that c-Src physically interacts with Her2 in breast carcinoma cell lines and related studies have shown that Src can phosphorylate Igf1r (44, 45). While additional studies are required to explore this possible mechanism of third party cross-talk, the observation of lapatinib-induced Igf1r phosphorylation highlights the potential importance of simultaneous targeting of Igf1r and Her2 as a therapeutic strategy.

In summary, we have shown that formation of Igf1r and Her2 heterodimers is one of the mechanisms of rapidly developing resistance to Igf1r inhibitors in rhabdomyosarcoma (an important mechanism, but perhaps not the only mechanism). Our results have also shown that there is a functional crosstalk between these 2 receptors in that IGF ligand leads to Her2 phosphorylation and that a Her2 inhibitor improves sensitivity to an Igf1r inhibitor. This study has clinical significance because Igf1r inhibitors are currently being used in clinical trials and because resistance to Igf1r inhibitors can be reasonably expected in current and future clinical trials. Our studies suggest that targeting both Igf1r and Her2 simultaneously may be a very promising approach in abrogating resistance to Igf1r inhibitors in rhabdomyosarcoma.

Disclosure of Potential Conflicts of Interest

C. Keller: Speakers' Bureau, Milennium, Novartis, GlaxoSmithKline; consultant/advisory board and ownership interest in Numira Biosciences.

Acknowledgments

The authors thank Novartis for kindly providing us NVP-AEW541.

Grant Support

This work was supported in part by an innovation award from Alex's Lemonade Stand Foundation and in part by 5R01CA133229 awarded to C. Keller. J. Abraham was supported by a training award from the Scott Carter foundation. The study was funded in part by the Hyundai Hope on Wheels program.

The costs of publication of this article were defrayed in part by the payment of page charges. This article must therefore be hereby marked *advertisement* in accordance with 18 U.S.C. Section 1734 solely to indicate this fact.

Received July 23, 2010; revised January 14, 2011; accepted January 24, 2011; published OnlineFirst March 29, 2011.

References

1. Pappo AS, Shapiro DN, Crist WM. Rhabdomyosarcoma. Biology and treatment. Pediatr Clin North Am 1997;44:953–72.
2. Arndt CA, Crist WM. Common musculoskeletal tumors of childhood and adolescence. N Engl J Med 1999;341:342–52.
3. Breneman JC, Lyden E, Pappo AS, Link MP, Anderson JR, Parham DM, et al. Prognostic factors and clinical outcomes in children and adolescents with metastatic rhabdomyosarcoma—a report from the Intergroup Rhabdomyosarcoma Study IV. J Clin Oncol 2003;21:78–84.
4. Williams BA, Williams KM, Doyle J, Stephens D, Greenberg M, Malkin D, et al. Metastatic rhabdomyosarcoma: a retrospective review of patients treated at the hospital for sick children between 1989 and 1999. J Pediatr Hematol Oncol 2004;26:243–7.
5. Rowinsky EK, Youssoufian H, Tonra JR, Solomon P, Burtrum D, Ludwig DL. IMC-A12, a human IgG1 monoclonal antibody to the insulin-like growth factor I receptor. Clin Cancer Res 2007;13:5549s–55s.
6. Minniti CP, Tsokos M, Newton WA Jr., Helman LJ. Specific expression of insulin-like growth factor-II in rhabdomyosarcoma tumor cells. Am J Clin Pathol 1994;101:198–203.
7. Scott J, Cowell J, Robertson ME, Priestley LM, Wadey R, Hopkins B, et al. Insulin-like growth factor-II gene expression in Wilms' tumour and embryonic tissues. Nature 1985;317:260–2.
8. El-Badry OM, Minniti C, Kohn EC, Houghton PJ, Daughaday WH, Helman LJ. Insulin-like growth factor II acts as an autocrine growth and motility factor in human rhabdomyosarcoma tumors. Cell Growth Differ 1990;1:325–31.
9. Blandford MC, Barr FG, Lynch JC, Randall RL, Qualman SJ, Keller C. Rhabdomyosarcomas utilize developmental, myogenic growth factors for disease advantage: a report from the Children's Oncology Group. Pediatr Blood Cancer 2006;46:329–38.
10. Ayalon D, Glaser T, Werner H. Transcriptional regulation of IGF-I receptor gene expression by the PAX3-FKHR oncoprotein. Growth Horm IGF Res 2001;11:289–97.
11. Haluska P, Shaw HM, Batzel GN, Yin D, Molina JR, Molife LR, et al. Phase I dose escalation study of the anti insulin-like growth factor-I receptor monoclonal antibody CP-751,871 in patients with refractory solid tumors. Clin Cancer Res 2007;13:5834–40.
12. Kalebic T, Tsokos M, Helman LJ. In vivo treatment with antibody against IGF-1 receptor suppresses growth of human rhabdomyosarcoma and down-regulates p34cdc2. Cancer Res 1994;54:5531–4.
13. Maloney EK, McLaughlin JL, Dagdigian NE, Garrett LM, Connors KM, Zhou XM, et al. An anti-insulin-like growth factor I receptor antibody that is a potent inhibitor of cancer cell proliferation. Cancer Res 2003;63:5073–83.
14. Scotlandi K, Manara MC, Nicoletti G, Lollini PL, Lukas S, Benini S, et al. Antitumor activity of the insulin-like growth factor-I receptor kinase inhibitor NVP-AEW541 in musculoskeletal tumors. Cancer Res 2005;65:3868–76.
15. Garcia-Echeverria C, Pearson MA, Marti A, Meyer T, Mestan J, Zimmermann J, et al. In vivo antitumor activity of NVP-AEW541-A novel, potent, and selective inhibitor of the IGF-IR kinase. Cancer Cell 2004;5:231–9.
16. Shapiro DN, Jones BG, Shapiro LH, Dias P, Houghton PJ. Antisense-mediated reduction in insulin-like growth factor-I receptor expression suppresses the malignant phenotype of a human alveolar rhabdomyosarcoma. J Clin Invest 1994;94:1235–42.
17. O'Hare T, Eide CA, Deininger MW. Bcr-Abl kinase domain mutations, drug resistance, and the road to a cure for chronic myeloid leukemia. Blood 2007;110:2242–9.
18. Rubin BP, Heinrich MC, Corless CL. Gastrointestinal stromal tumour. Lancet 2007;369:1731–41.
19. Al-Batran SE, Hartmann JT, Heidel F, Stoehlmacher J, Wardelmann E, Dechow C, et al. Focal progression in patients with gastrointestinal stromal tumors after initial response to imatinib mesylate: a three-center-based study of 38 patients. Gastric Cancer 2007;10:145–52.
20. Chin L, DePinho RA. Flipping the oncogene switch: illumination of tumor maintenance and regression. Trends Genet 2000;16:147–50.

Published OnlineFirst March 29, 2011; DOI:10.1158/1535-7163.MCT-10-0695

21. Keller C, Arenkiel BR, Coffin CM, El-Bardeesy N, DePinho RA, Capecchi MR. Alveolar rhabdomyosarcomas in conditional Pax3:Fkhr mice: cooperativity of Ink4a/ARF and Trp53 loss of function. Genes Dev 2004;18:2614–26.
22. Taniguchi E, Nishijo K, McCleish AT, Michalek JE, Grayson MH, Infante AJ, et al. PDGFR-A is a therapeutic target in alveolar rhabdomyosarcoma. Oncogene 2008;27:6550–60.
23. Nishijo K, Chen QR, Zhang L, McCleish AT, Rodriguez A, Cho MJ, et al. Credentialing a preclinical mouse model of alveolar rhabdomyosarcoma. Cancer Res 2009;69:2902–11.
24. Nishijo K, Hosoyama T, Bjornson CR, Schaffer BS, Prajapati SI, Bahadur AN, et al. Biomarker system for studying muscle, stem cells, and cancer in vivo. Faseb J 2009;23:2681–90.
25. Frasca F, Pandini G, Scalia P, Sciacca L, Mineo R, Costantino A, et al. Insulin receptor isoform A, a newly recognized, high-affinity insulin-like growth factor II receptor in fetal and cancer cells. Mol Cell Biol 1999;19:3278–88.
26. Corless CL, Schroeder A, Griffith D, Town A, McGreevey L, Harrell P, et al. PDGFRA mutations in gastrointestinal stromal tumors: frequency, spectrum and in vitro sensitivity to imatinib. J Clin Oncol 2005;23:5357–64.
27. Engelman JA, Zejnullahu K, Mitsudomi T, Song Y, Hyland C, Park JO, et al. MET amplification leads to gefitinib resistance in lung cancer by activating ERBB3 signaling. Science 2007;316:1039–43.
28. Kumabe T, Sohma Y, Kayama T, Yoshimoto T, Yamamoto T. Over-expression and amplification of alpha-PDGF receptor gene lacking exons coding for a portion of the extracellular region in a malignant glioma. Tohoku J Exp Med 1992;168:265–9.
29. Sihto H, Sarlomo-Rikala M, Tynninen O, Tanner M, Andersson LC, Franssila K, et al. KIT and platelet-derived growth factor receptor alpha tyrosine kinase gene mutations and KIT amplifications in human solid tumors. J Clin Oncol 2005;23:49–57.
30. Martins AS, Ordonez JL, Garcia-Sanchez A, Herrero D, Sevillano V, Osuna D, et al. A pivotal role for heat shock protein 90 in Ewing sarcoma resistance to anti-insulin-like growth factor 1 receptor treatment: in vitro and in vivo study. Cancer Res 2008;68:6260–70.
31. Huang F, Greer A, Hurlburt W, Han X, Hafezi R, Wittenberg GM, et al. The mechanisms of differential sensitivity to an insulin-like growth factor-1 receptor inhibitor (BMS-536924) and rationale for combining with EGFR/HER2 inhibitors. Cancer Res 2009;69:161–70.
32. Huang F, Hurlburt W, Greer A, Reeves KA, Hillerman S, Chang H, et al. Differential mechanisms of acquired resistance to insulin-like growth factor-i receptor antibody therapy or to a small-molecule inhibitor, BMS-754807, in a human rhabdomyosarcoma model. Cancer Res 2010;70:7221–31.
33. Haluska P, Carboni JM, TenEyck C, Attar RM, Hou X, Yu C, et al. HER receptor signaling confers resistance to the insulin-like growth factor-I receptor inhibitor, BMS-536924. Mol Cancer Ther 2008;7:2589–98.
34. Nahta R, Esteva FJ. HER2 therapy: molecular mechanisms of trastuzumab resistance. Breast Cancer Res 2006;8:215.
35. Nahta R, Yuan LX, Zhang B, Kobayashi R, Esteva FJ. Insulin-like growth factor-I receptor/human epidermal growth factor receptor 2 heterodimerization contributes to trastuzumab resistance of breast cancer cells. Cancer Res 2005;65:11118–28.
36. Camirand A, Lu Y, Pollak M. Co-targeting HER2/ErbB2 and insulin-like growth factor-1 receptors causes synergistic inhibition of growth in HER2-overexpressing breast cancer cells. Med Sci Monit 2002;8:BR521–6.
37. Desbois-Mouthon C, Cacheux W, Blivet-Van Eggelpoel MJ, Barbu V, Fartoux L, Poupon R, et al. Impact of IGF-1R/EGFR cross-talks on hepatoma cell sensitivity to gefitinib. Int J Cancer 2006;119:2557–66.
38. Lu Y, Zi X, Pollak M. Molecular mechanisms underlying IGF-I-induced attenuation of the growth-inhibitory activity of trastuzumab (Herceptin) on SKBR3 breast cancer cells. Int J Cancer 2004;108:334–41.
39. Gooch JL, Van Den Berg CL, Yee D. Insulin-like growth factor (IGF)-I rescues breast cancer cells from chemotherapy-induced cell death–proliferative and anti-apoptotic effects. Breast Cancer Res Treat 1999;56:1–10.
40. Romond EH, Perez EA, Bryant J, Suman VJ, Geyer CE Jr., Davidson NE, et al. Trastuzumab plus adjuvant chemotherapy for operable HER2-positive breast cancer. N Engl J Med 2005;353:1673–84.
41. Piccart-Gebhart MJ, Procter M, Leyland-Jones B, Goldhirsch A, Untch M, Smith I, et al. Trastuzumab after adjuvant chemotherapy in HER2-positive breast cancer. N Engl J Med 2005;353:1659–72.
42. Buzdar AU, Ibrahim NK, Francis D, Booser DJ, Thomas ES, Theriault RL, et al. Significantly higher pathologic complete remission rate after neoadjuvant therapy with trastuzumab, paclitaxel, and epirubicin chemotherapy: results of a randomized trial in human epidermal growth factor receptor 2-positive operable breast cancer. J Clin Oncol 2005;23:3676–85.
43. Balana ME, Labriola L, Salatino M, Movsichoff F, Peters G, Charreau EH, et al. Activation of ErbB-2 via a hierarchical interaction between ErbB-2 and type I insulin-like growth factor receptor in mammary tumor cells. Oncogene 2001;20:34–47.
44. Belsches-Jablonski AP, Biscardi JS, Peavy DR, Tice DA, Romney DA, Parsons SJ. Src family kinases and HER2 interactions in human breast cancer cell growth and survival. Oncogene 2001;20:1465–75.
45. Peterson JE, Kulik G, Jelinek T, Reuter CW, Shannon JA, Weber MJ. Src phosphorylates the insulin-like growth factor type I receptor on the autophosphorylation sites. Requirement for transformation by src. J Biol Chem 1996;271:31562–71.

Supplementary Material

Supplementary Materials and Methods:

Gene expression analysis: For gene expression studies in mice, total RNA was extracted from tumor samples using TRIZOL according to the manufacturer's instructions (Invitrogen, Carlsbad, CA). RNA was then purified using Qiagen RNeasy miniprep cleanup kit per manufacturer instructions (Qiagen, Valencia, CA). cDNA was generated using oligo-dT primers as previously described (1). Real time PCR (RT-PCR) was then performed on an ABI Prism 7500 Fast Real-Time PCR system using SYBR Green PCR Master mix according to the manufacturer's recommendations (Applied Biosystems, Foster City, CA). The following primers were used: mouse *Igf2-r* (5'-CTGGAGGTGATGAGTGTAGCTCTGGC-3'and 5'-GAGTGACGAGCCAACACAGACAGGTC-3'), mouse *Igf1* (5'-GGACCAGAGACCCTTTGCGGGG-3'and 5'-GGCTGCTTTTGTAGGCTTCAGTGG-3'), mouse *Igf1r* (5'-GCTTCGTTATCCACGACGATG-3' and 5'-GAATGGCGGATCTTCACGTAG-3'), mouse *Igf2* (5'-GTCGATGTTGGTGCTTCTCATC-3' and 5'-GGGTATCTGGGGAAGTCGT-3'), mouse *IR-A* and *IR-B* isoforms (5'-CAGAAGCACAATCAGAGTGAG-3' and 5'-GTGTGGTGGCTGTCACATTC-3'). Expression of gene products was normalized to levels of *GAPDH*. Primer sequences for mouse *GAPDH* were: 5'-TGCACCACCAACTGCTTAG-3'and 5'-GGATGCAGGGATGATGTTC-3'. For human samples, RT-PCR was performed by using TaqMan probes as previously described (2). Expression levels in human tumors were reported previously (2) but comparison to skeletal muscle expression is newly reported here.

RNA-interference: Unpooled mouse *Igf1r* siRNA (Cat# J-056843-06; Dharmacon, Lafayette, CO) was transfected into mouse tumor cells using Lipofectamine-2000 (Invitrogen). The cells were incubated with *Igf1r* siRNA for 6 days, after which the cells were lysed and the lysate was used for western blot analysis. Scrambled siRNA (Dharmacon) was used a control.

Supplementary Figure Legends:

Figure S1. Chemical structures for compounds in this study (a) NVP-AEW541 (b) Lapatinib.

Figure S2. Characterization of CAM assay properties. (a) Standard curve showing a concomitant increase in bioluminescence signal with the increase in the number of tumor cells growing on a quail CAM. (b) Average weight of

quail embryos three days after tumor cells on a 3D scaffold were placed on quail CAMs and treated with vehicle (DMSO) or drugs (Imatinib, NVP-AEW541).

Figure S3: Quantitative RT-PCR showing increased mRNA levels of *Igf1r* in human and mouse alveolar rhabdomyosarcoma**.** (a) *Igf1r* and *Igfr2* along with their ligand *Igf2* are over expressed in human ARMS and ERMS compared to normal skeletal muscle [top panel]. (b) *Igf1r*, *Igf2 and Igf2r* are highly expressed in the primary tumors compared to the normal skeletal muscle in the mouse model of alveolar rhabdomyosarcoma. The *Igf1 receptor* not only is highly expressed in the primary tumors but also in metastatic tumors [bottom panel].

Figure S4: *Igf1r* siRNA treatment inhibits cell proliferation and phosphorylation of Igf1r and downstream mediators. (a) Cell viability assay performed on naive rhabdomyosarcoma primary cell cultures (U21089) treated with *Igf1r* siRNA. (b) Immunoblots showing that treatment of mouse rhabdomyosarcoma cell line (U21089) with 100nm *Igf1r* siRNA causes a reduction in the phosphorylation of Igf1r, Mapk, Akt, IRS1 and P70 S6 kinase.

Supplementary References:

1. Nishijo K, Chen QR, Zhang L, McCleish AT, Rodriguez A, Cho MJ, et al. Credentialing a preclinical mouse model of alveolar rhabdomyosarcoma. Cancer Res. 2009;69:2902-11.
2. Blandford MC, Barr FG, Lynch JC, Randall RL, Qualman SJ, Keller C. Rhabdomyosarcomas utilize developmental, myogenic growth factors for disease advantage: a report from the Children's Oncology Group. Pediatr Blood Cancer. 2006;46:329-38.

Supplementary Figure S1

A

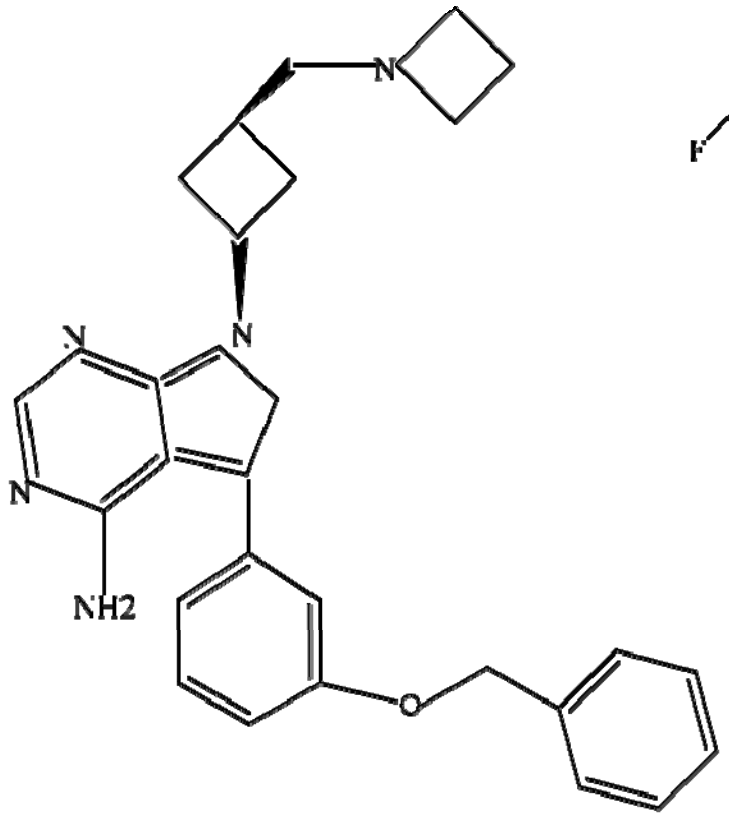

NVP-AEW541

B

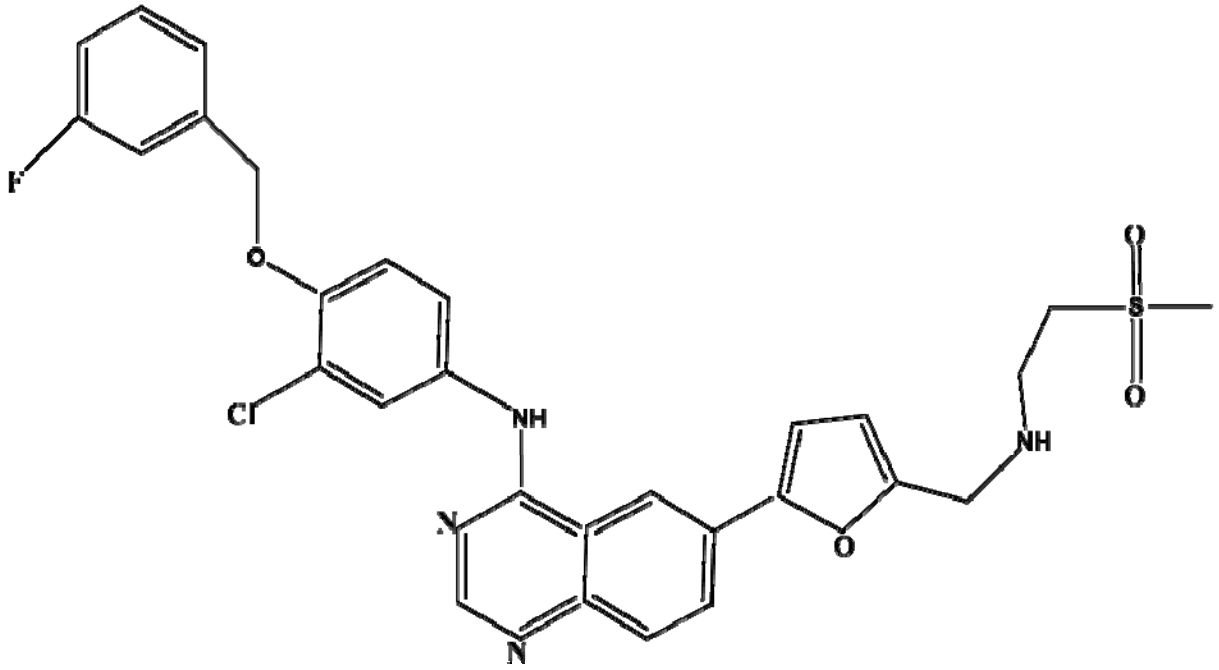

Lapatinib

Supplementary Figure S2

A

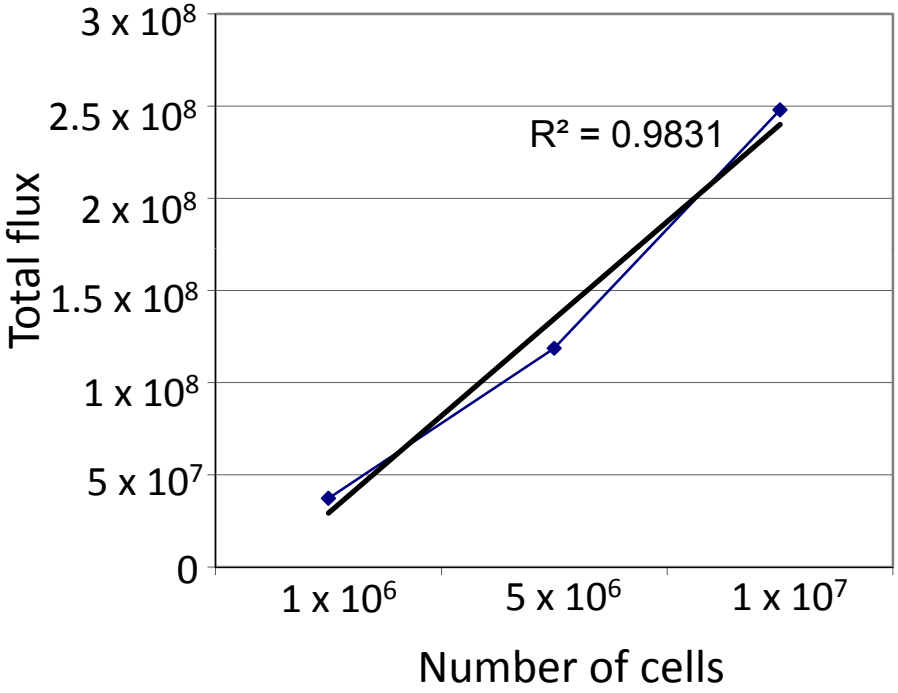

B

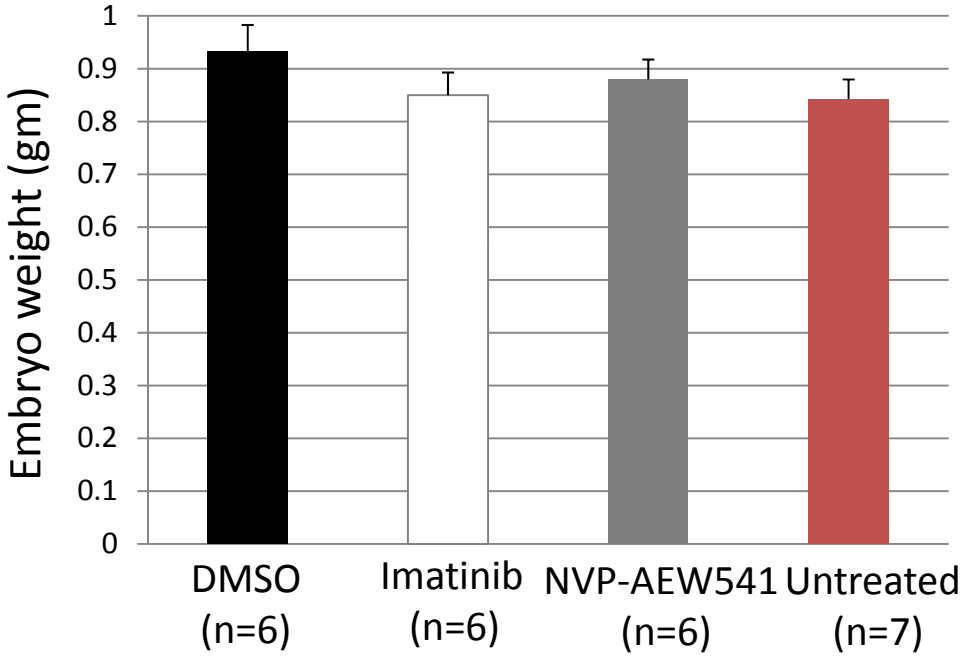

Supplementary Figure S3

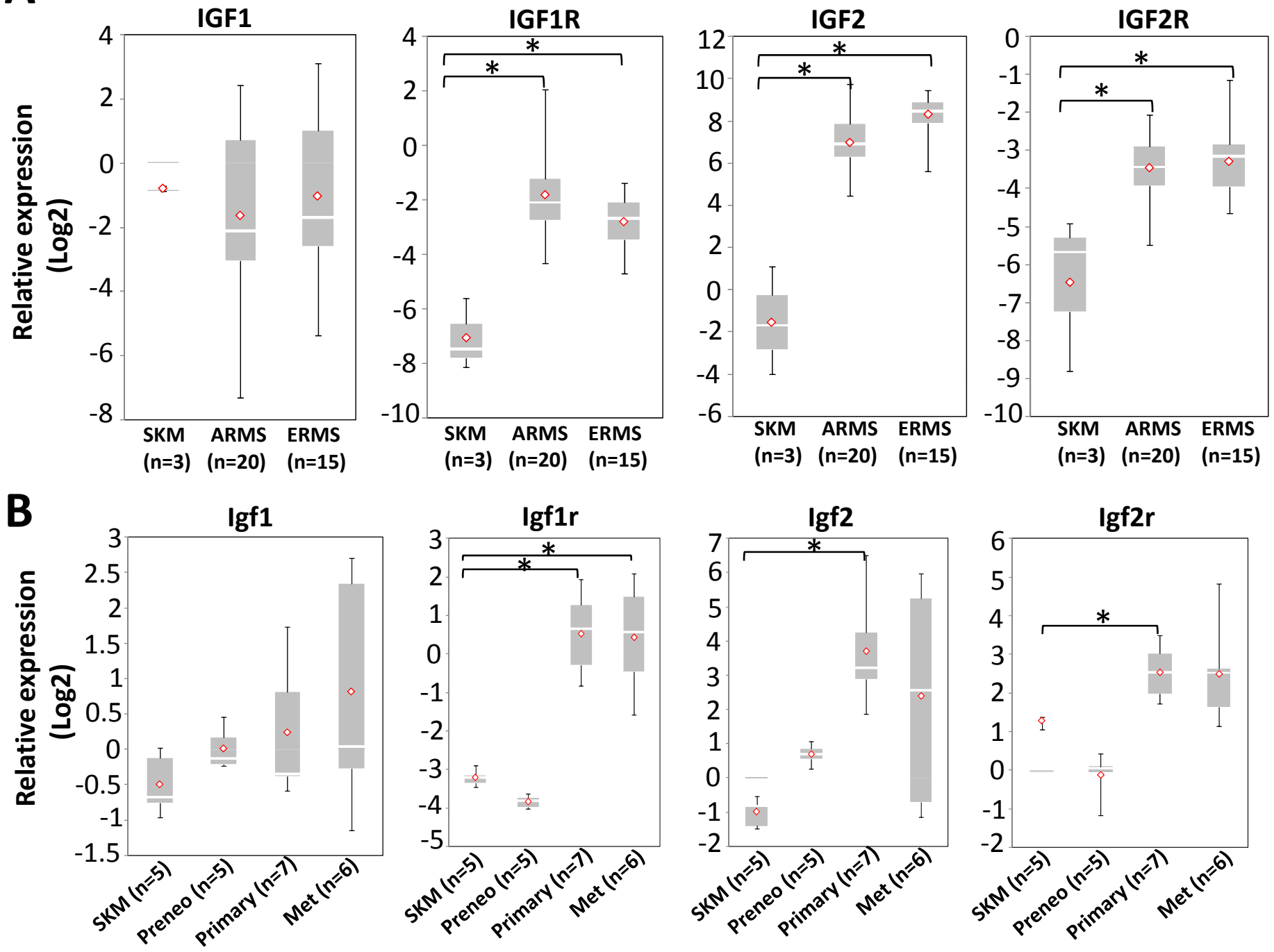

Supplementary Figure S4

A

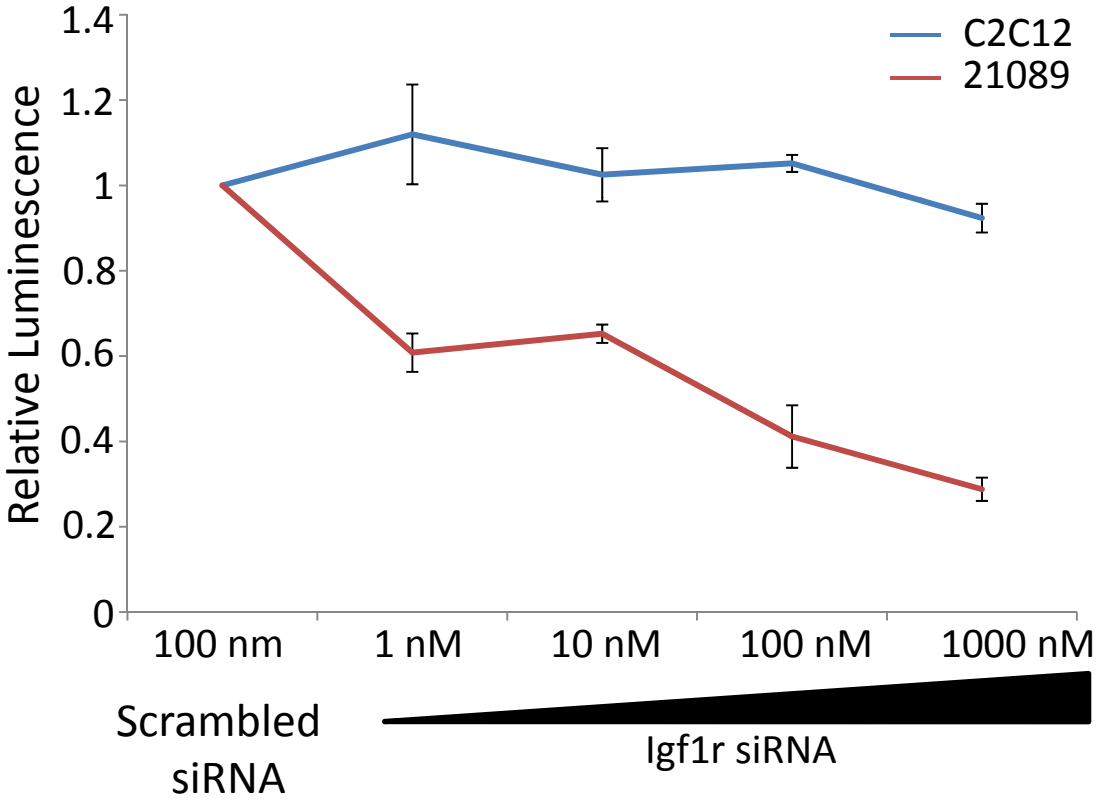

B

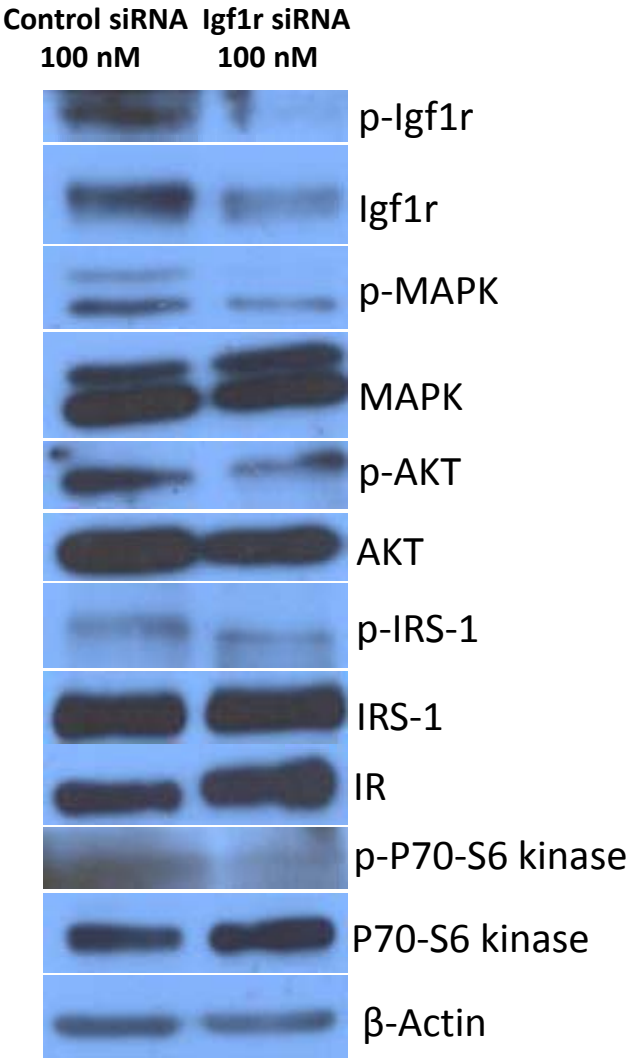

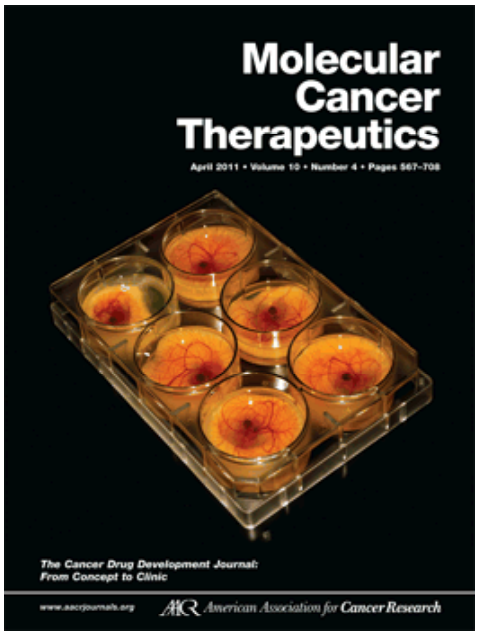

Cover image

Genetically-engineered mouse models often represent some of the most physiologically accurate models of cancer from which to understand the tumor microenvironment and with which to perform preclinical trials. Abraham and colleagues present studies of a prototypic insulin-like growth factor receptor inhibitor using both genetically-engineered mouse models and the shell-free quail chorioallantois membrane (CAM) assay. Remarkably, the inexpensive short term (2 week) CAM assay offers xenografted tumors a scaffold of lymphatics, arteries, and veins that mimic short-term ***in vivo*** growth with all the advantages of intravital imaging. Photograph credits, Elaine Huang and Audra Lee. For details, see article by Abraham and colleagues on page 697.